CHAPTER

11

Conformational Restriction and Steric Hindrance in Medicinal Chemistry

Peter Wipf[1], *Erin M. Skoda*[1] *and André Mann*[2]

[1]Department of Chemistry, University of Pittsburgh, Pittsburgh PA, USA; [2]LAAS-CNRS, Université Louis Pasteur, Strasbourg, France

OUTLINE

I. INTRODUCTION

For the practice of medicinal chemistry, an understanding of the thermodynamics of molecular recognition processes is essential. Noncovalent interactions between a ligand and a protein are mediated by several parameters. Ion–ion, dipole–dipole, and ion-dipole forces, hydrophobicity, hydrogen bonding, and shape complementarity play significant roles. The magnitude of the binding equilibrium is determined by the thermodynamic contributions of each of these interactions. When two molecules bind, their binding energy must compensate for their desolvation— in most cases the removal of all or part of their water shell. The probability that a ligand is trapped in a receptor is dependent on the promotion of binding by favorable interactions of polar functional groups and the formation of hydrophobic contacts. In addition to desolvation, adverse factors for binding are mainly related to the restriction of translational and vibrational energies upon complex formation [1–4]. While the ligand generally loses conformational freedom, the entropy of the solvent increases. In order to overcome entropy penalties and improve the binding affinity of a ligand, a suitable strategy is to restrict its conformational flexibility. Therefore, once a lead compound has been identified for a targeted biological receptor, the optimization toward potency and/or selectivity usually involves the modification of its conformation. Depending on the chemical structure of the identified lead, conformational restriction and/or steric hindrance can be introduced by adding or removing key bonds and substituents. An optimization of the free energy released during the association of a ligand with a receptor can be achieved by modifying the spatial disposition of functional groups through steric strain, hybridization, or cyclization. The expected benefits are receptor selectivity, potency increase, pharmacophore optimization, and metabolic stabilization. As a bonus, this strategy can be expected to produce original compounds and innovative chemistry. Finally, there are also some risks: any structural change

in a compound alters more than one property and can have unexpected consequences. Indeed, this approach is valuable in cases where the lead compounds are exhibiting flexibility and where the low-energy conformations are not representative for a good fit to the receptor. In this chapter, some theoretical points related to the thermodynamic aspects of lead optimization will be addressed, and then several examples will be presented where the modification of rigidity has had an impact in drug design.

A. Theoretical Aspects of Ligand Binding

Molecular recognition is a key factor in all biological processes. Accordingly, many of the important issues in medicinal chemistry hinge on an understanding of the noncovalent interactions between a biomacromolecule (receptor) and a small ligand (drug). Under equilibrium conditions, the binding affinity can be expressed in terms of the difference in free energy (ΔG°) of free and bound states or the equilibrium constant (K), which are correlated by the Gibbs-van't Hoff equation (Eq. 11.1):

$$\Delta G^\circ = -RT \ln K \quad \{\text{with } \Delta G^\circ = \Delta H^\circ - T\Delta S^\circ; \mathrm{R} = 8.13\ \mathrm{J/mol/K}\} \tag{11.1}$$

The more negative ΔG°, the stronger is the binding of the ligand to the bioreceptor (the binding constant is large). As a reminder, if a noncovalent association is expected, ΔG° must be negative and the Gibbs equation usually contains a negative value for ΔH° and a positive value for $T\Delta S^\circ$. If $\Delta G^\circ = -30$ kJ/mol, the association constant is in the micromolar range. By using the Gibbs equation, we can distinguish between the effects of functional group interactions within the complex (ΔH°) and changes in the entropy upon binding ($T\Delta S^\circ$). The values of the standard free enthalpy ΔH° can serve as a quantitative indicator of the changes in intermolecular bond energies (mainly hydrogen bonding and van der Waals interactions) occurring during the binding, while the standard free entropy ΔS° is a good indicator of the reorganization in the solvation shell and the conformational changes during the same process. Only a negative ΔG° favors the equilibrium of the association. While in the formation of a covalent bond, ΔH° usually has the major contribution to ΔG°, in the case of a noncovalent interaction or equilibrium, the contributions by ΔH° and $T\Delta S^\circ$ to the free energy are often comparable. Given the large bond strengths of 300 to 500 kJ/mol for covalent bonds and the prevalence of the enthalpy term ($\Delta H^\circ >> T\Delta S^\circ$), the much smaller energy of 1 to 60 kJ/mol released in a reversible interaction is composed of roughly equivalent enthalpy and entropy terms ($\Delta H^\circ \cong T\Delta S^\circ$) [5–8] (Figure 11.1).

The binding energy values for noncovalent associations are small and comparable to the solvation energies that oppose them in the binding event in aqueous media. Binding constants have been estimated by taking advantage of the Gibbs equation. Böhm used a set of interactions arising from experimentally determined binding constants resulting from the association of small organic molecules with proteins [10]. Five types of ΔG° contributions were identified (Table 11.1) and their values were extracted from a regression analysis. These values are generally used for a semi-quantitative evaluation of binding constants and can be applied in ligand optimization.

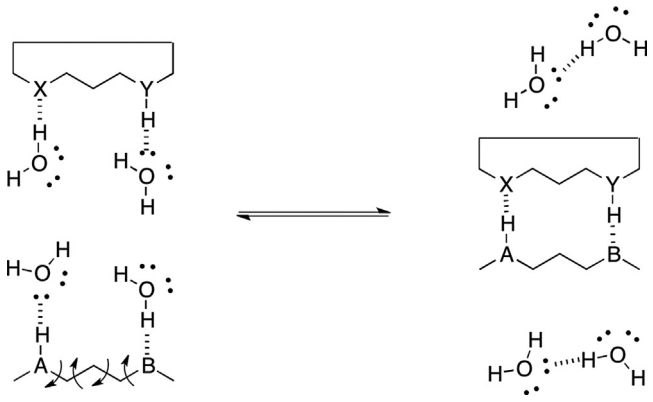

FIGURE 11.1 Noncovalent association between a ligand with two polar atoms (A and B) linked by a 3-carbon chain with a receptor containing complementary functions (X and Y), with the dashed line indicating hydrogen bonding [9].

TABLE 11.1 Average Values for ΔG° Contributions [9,10]

Physical process	ΔG° (kJ/mol)
Energy cost of bimolecular association	+5.4
Energy cost of restriction of an internal rotor	+2.0 (per rotor)
Hydrophobic effect (per Å of buried hydrocarbon)	−0.17/Å
Benefit of forming a neutral hydrogen bond of ideal geometry	−4.7
Benefit of forming an ionic hydrogen bond of ideal geometry	−8.3

1. Enthalpy–Entropy Compensation

A key factor that needs to be considered in the analysis of binding events is that a decrease in motion implies a decrease in entropy, since it results in fewer accessible arrangements. Consider the formation of a specific noncovalent bond (e.g., L···R for the transformation L + R → L···R). An increase in its strength (which corresponds to an additional negative contribution to ΔH°, favorable to the binding process) will be accompanied by an increasing restriction in the molecular motion of L and R in L···R (which corresponds to a decrease in ΔS°, unfavorable to the binding process). This opposing interplay between enthalpy and entropy is known as enthalpy–entropy compensation and represents a fundamental property of noncovalent interactions [11,12]. It arises because bonding opposes motion and, reciprocally, motion opposes bonding. The two effects can be compromised because the strength of noncovalent bonds at room temperature is comparable to kT, the product of the Boltzmann constant and the temperature. The thermodynamic parameters (ΔG°, ΔH°, ΔS°) for 136 ligands binding to ten biological receptors (mainly membrane receptors) have been analyzed [12]. It appeared that ΔH° and $T\Delta S^\circ$ values show a linear correlation (Eq. 11.2). This relationship seems remarkable in view of its high correlation and statistical relevance (n = 186). The observed enthalpy–entropy compensation seems to reflect general principles of the binding processes, irrespective of the nature of ligands and of their macromolecular targets:[12]

$$\Delta H^\circ = -40\ \text{kJ mol}^{-1} + 278\ \Delta S^\circ (\text{in kJ K}^{-1}\text{mol}^{-1}) \quad (n = 186, R^2 = 0.981, P \leq 0.001) \tag{11.2}$$

This linear correlation reflects another concept: any tightening of the intermolecular bonds (the enthalpic contribution) is compensated by a loss of degrees of freedom (the entropic contribution). The binding association can be enthalpy- or entropy-driven. The origin of the $\Delta H/\Delta S$ compensation is probably related to an intrinsic property of the hydrogen bond, which determines the association of the participants (water, drug, and binding site) in the drug-receptor binding equilibrium [11,12]. Accordingly, the thermodynamic laws teach us that three factors are involved in improving binding affinity: (1) improving ligand-protein interactions over those with the solvent in order to obtain a favorable (negative) enthalpy change; (2) increasing the hydrophobicity of the ligand in order to displace solvent molecules in the binding site and increase entropy; and (3) pre-shaping the ligand to complement the geometry of the binding site in order to minimize the loss of conformational entropy upon binding [13].

2. Enthalpy- Versus Entropy-Driven Binding

The following example is illustrative for the $\Delta H/\Delta S$ compensation. The binding of a series of agonists and antagonists of the β-adrenergic receptor displays thermodynamic differences between agonists and antagonists (Table 11.2) [14,15]. β-Adrenergic agonists and/or partial agonists are found to bind with large negative enthalpies (ΔH° from −79 to −17 kJ/mol), indicating strong electrostatic interactions between the bound conformation on the receptor, associated with a large loss of entropy (a tight complex is formed: $T\Delta S^\circ$ from −45.8 to + 8.6 kJ/mol). Antagonists, on the other hand, do not fulfill the requirements of a good complementarity as evidenced by the criterion that their enthalpies of binding are small (ΔH° from −21.3 to + 16.4 kJ/mol): The loss of entropy through conformational restriction is therefore less than that of the agonists, and—in fact—the entropy change is positive upon binding ($T\Delta S^\circ$ from +16.9 to + 52.5 kJ/mol). Overall, agonists and antagonists have similar association constants, supporting the $\Delta H^\circ/\Delta S^\circ$ compensation paradigm (Table 11.2).

In order to improve our understanding of the $\Delta H^\circ/\Delta S^\circ$ compensation, the data from Table 11.2 are represented with a plot of ΔH° versus $T\Delta S^\circ$. Indeed, in Figure 11.2, clusters clearly differentiate agonists from antagonists or partial agonists. An interesting explanation based on the dimerization of the membrane-bound receptors (G-protein-coupled receptors) has been given by Williams:[8] the agonists (●; activating the receptor after

TABLE 11.2 Thermodynamic Parameters of Ligand Binding to the β-Adrenergic Receptor of Turkey Erythrocytes and Ratio of Equilibrium Constants K_D at 0°C and 37°C [14]

	ΔG° (kJ/mol)	ΔH° (kJ/mol)	ΔS° (J/mol deg)	$T\Delta S^\circ$ (kJ/mol)	K_D (37°C)/ K_D (0 °C)
AGONISTS					
(−)-isoproterenol	− 39.3	− 56.0	− 54.0	− 16.7	23
(−)-norephedrine	− 33.1	− 78.9	− 147.7	− 45.8	55
PARTIAL AGONISTS					
soteronol	− 34.4	− 32.8	+ 5.3	+ 1.6	5.3
fenoterol	− 32.7	− 25.4	+ 23.6	+ 7.3	3.6
terbutaline	− 25.9	− 17.3	+ 27.8	+ 8.6	2.4
ANTAGONISTS					
(−)-propranolol	− 52.3	− 16.1	+ 116.7	+ 36.2	2.6
IPS-339	− 51.5	+ 1.1	+ 169.5	+ 52.5	0.95
pindolol	− 49.6	− 21.3	+ 91.2	+ 28.3	3.0
sotalol	− 34.4	− 9.0	+ 81.6	+ 25.3	1.6
atenolol	− 31.3	− 14.5	+ 54.4	+ 16.9	2.1
practolol	− 31.2	+ 16.4	+ 153.6	+ 47.6	0.45

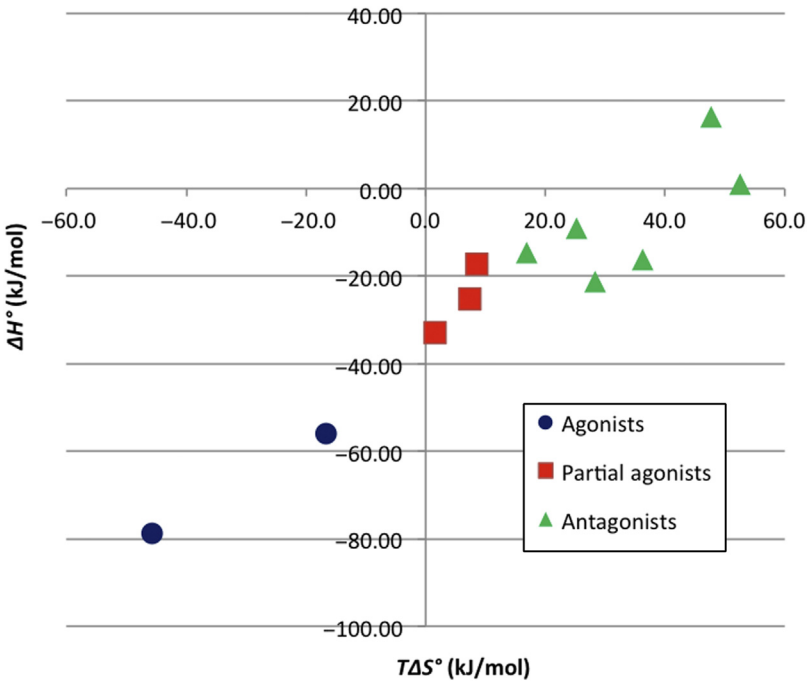

FIGURE 11.2 Plot of ΔH° versus $T\Delta S^\circ$ for the binding of agonists (●), antagonists (▲), and partial agonists (■) to the β-adrenergic receptors. *Data from Table 11.2 were used [14].*

binding) induce receptor aggregation, which is beneficial in bonding (negative contribution to ΔH°) but adverse in entropy (negative contribution to $T\Delta S^\circ$). The antagonist (▲; without activation after binding) should therefore be (in comparison to agonist binding) relatively disfavoring for dimerization and entropy. The consequences are seen in Figure 11.2. The agonists (●) are binding to the β-receptors by an enthalpy-driven process, whereas the antagonists (▲) are binding with entropy and/or enthalpy−entropy-driven processes.

In contrast, if agonists induce dissociation of receptor oligomers (e.g., the adenosine A1 or A2 receptors) [8,16], antagonists may induce the formation of oligomers. Such antagonist binding should therefore be (in comparison to agonist binding) relatively favorable in overall enthalpy and unfavorable in entropy, in contrast to the agonists with adverse enthalpy and favorable entropy.

Finally, an important point to stress is that hydrophobicity is a major source of binding in drug-receptor interactions. Based on a study of over 415 oral drugs, it appeared that on average drugs contain only one to two hydrogen donors and three to four acceptors, whereas the average number of hydrophobic atoms in a drug is 16 [17]. The contributions of polar and hydrophobic interactions in molecular recognition are related to the balance of enthalpy and entropy.

B. Steric Constraints

Before a small ligand interacts with a biological receptor, the two entities have their separate translational and rotational flexibility, which contribute to their respective entropy. Once the association occurs, some degrees of motion as well as internal rotations around single bonds are lost, and the consequence is an entropy cost of about -58 kJ/mol for a small ligand (MW $<$ 1,000 Da) at room temperature [4,7,8]. As a general consequence of the binding of a ligand to a receptor, entropy is decreased due to the loss of degrees of motion when two molecules are rigidly constrained within a complex. The torsional contribution to the entropy (the free rotation of a bond) is related to the number of rotatable bonds in the ligand, and freezing one of them has a cost of 2–3 kJ/mol at room temperature [4,7,9]. Considering Equation 11.1, the entropy penalty will render ΔS negative, reducing the binding energy. In order for $\Delta G^\circ < 0$, the costs in reducing conformational flexibility must be offset by favorable intermolecular interactions such as hydrogen bonds, van der Waals packing, hydrophobic interactions, and Coulombic interactions. One consequence of this effect is that the binding optimization of a flexible ligand can be accomplished by making ΔH° more negative, by making ΔS° more positive, or by an appropriate combination of both. Theoretically, the highest value for a given binding constant is accessible to a flexible ligand if the receptor recognizes the ligand in its low-energy conformation that presents an optimal orientation of the functional groups. Therefore, all information gained about the active conformation of the ligand will serve the chemical design of a better lead structure. Some illustrative examples can be obtained from the incorporation of constrained amino acids into bioactive compounds [18]. However, since the determination of the thermodynamic parameters of ligand/receptor interactions is still in its infancy, optimizations in structure-based drug design rely on semi-quantitative and empirical strategies and structure–activity relationships (SAR). Conformational constraints, steric hindrance, and rigidification are frequently used principles in medicinal chemistry to explore binding parameters. Phenylalanine, a lipophilic amino acid, has been a popular substrate for evaluating this concept of rigidification. Nonnatural phenylalanine analogs have been synthesized by the introduction of bulky substituents, by the application of carbocyclic constraints, or by the incorporation of a functional group. Examples of conformationally constrained phenylalanine analogs are shown in Figure 11.3 [19–22].

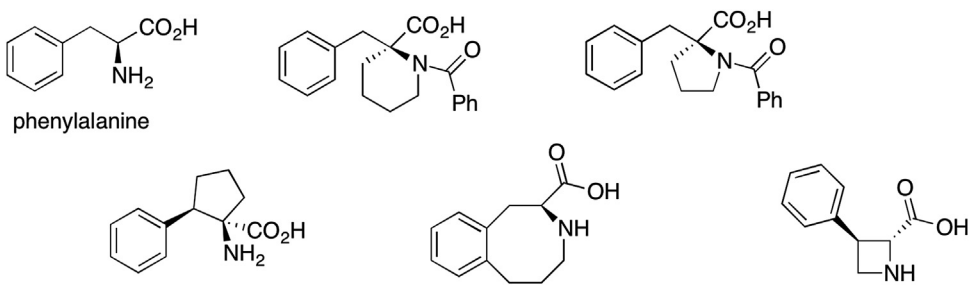

FIGURE 11.3 Conformational rigidification of phenylalanine analogs [19–22].

C. Conformational Analysis

Many computational methods are available to determine the low-energy conformations of a flexible ligand [23–25]. During the binding process, flexible ligands are refolded. This refolding is a general phenomenon and is presumably compensated by the search of a ligand for hydrogen bonds on the protein to replace the solute-solvent hydrogen bonds that are lost as the molecule enters the binding site (as shown in Figure 11.1) or in the unmasking of hydrophobic pockets on the receptor. A study has been performed on thirty-three ligands whose X-ray structures as well as conformations obtained by co-crystallization with their receptors have been recorded [26]. From this study, it appears that the degree of conformational change depends in part on the number of rotatable bonds in the ligand. For ligands with five or more rotatable bonds, the conformation in the crystal

structure does not represent the protein-bound conformation. Therefore, the solid-state structure of flexible ligands remains often of limited use for SAR analyses. Of course, in the more favorable cases, when a crystal structure of the complex-ligand−receptor can be obtained, the design of an improved ligand is facilitated because the main interactions can be recognized and then further optimized via synthesis.

D. Steric Effects

Steric effects may arise in a number of ways. Primary steric effects result from repulsions between valence electrons or nonbonded atoms. Such repulsions can only result in an increase in the energy of the system. In a chemical reaction, the overall steric effect may be either favorable or unfavorable. For example, if steric effects in the reactant are larger than in the product (or transition state), then the reaction is favored (steric augmentation); if the reverse case is true, the reaction is disfavored (steric diminution). The same arguments can be used in biological systems for the formation of a receptor−ligand complex. Comparing the binding of a ligand to a biological receptor with or without a subsequent chemical reaction—for example, an enzyme or a hormonal receptor—reveals some obvious differences. The enzymatic reactions involve only substructures in proximity to those atoms that are actually participating in bond making or breaking. Therefore, the enzyme tolerates structurally different ligands, provided the position on the substrate where the reaction should take place is accessible. Even if the direct affinity of a ligand for an enzyme is low, the subsequent chemical transformation can take place. In the formation of a ligand−receptor complex, any group of atoms that is in van der Waals contact with the receptor or the biomolecule can be or is involved in the binding event. If the receptor sits in a pocket that can adjust to any bioactive substance no matter its size or shape, then no steric effect will be observed. If, however, the parent biopolymer has limited conformational flexibility, and—as is likely—this flexibility is not equivalent in all directions, then a steric effect will be observed. Furthermore, the steric effect will be dependent on conformational states, and the minimal steric interaction principle will probably be observed. This principle states that a substituent whose steric effect is conformationally variable will prefer a conformation that minimizes steric repulsions and will give rise to the smallest steric strain. Finally, there are secondary steric effects on receptor binding that are produced by a substituent: (1) lowering the accessibility to an important group due to steric hindrance; (2) changing the population of a conformer due to steric effects; (3) shielding the active site from attack by a bulky group; and (4) variation in the electronic resonance of a π-bonded substituent by an out-of-plane repulsion.

E. Rigid Compounds and Bioavailability

Any effort toward improving bioavailability is of great importance in the drug discovery process. An intriguing correlation between the bioavailability of a compound and the number of its rotatable bounds was reported by Veber and coworkers using an empirical approach based on a set of 1,100 drug candidates and metabolism data collected from rats [27]. Remarkably, 10 or fewer rotatable bonds together with a polar surface area <140 $Å^2$ (or 12 or fewer H-bond donors and/or acceptors) irrespective of the molecular weight resulted in a high probability for good oral bioavailability in rats. This finding expanded the acceptable range of molecular weight values for a drug candidate beyond the threshold of 500 g/mol set by the Lipinski rules [28]. Veber suggested that by freezing some of the rotatable bounds, the molecular weight was no longer an essential parameter to be considered. The extent to which the number of rotatable bonds, as compared to other physicochemical parameters, affects oral bioavailability was recently also analyzed by Varma and coworkers [29]. Oral bioavailability (F) depends on the fraction of compound absorbed (F_a) as well as first-pass elimination that is determined by the fraction escaping gut-wall elimination (F_g) and the fraction escaping hepatic elimination (F_h), as shown in Equation 11.3. Each of the parameters evaluated (molecular weight, ionization state, lipophilicity, polar surface area, and rotatable bonds) affected at least one aspect of oral bioavailability. For example, while increasing molecular weight caused a decrease in F_a, increasing lipophilicity caused a decrease in F_g and F_h. Most notably, increasing the number of rotatable bonds had a negative effect on all three parameters and profoundly affected oral bioavailability [29]. Therefore, the introduction of conformational constraints in a drug candidate also has to be considered for resolving pharmacokinetic issues.

$$F = F_a \times F_g \times F_h \tag{11.3}$$

II. CASE STUDIES

A. The Study of Receptor Structure

A classic example of exploring the structure and binding requirements of a target enzyme by conformational restriction without the benefit of a co-crystal structure is presented by the μ-opioid receptor antagonists. Drugs that have been approved to target this receptor are used for pain management, and the name of the receptor family is derived from the prototypical antagonist of this family, morphine. Activation of the μ-opioid receptor family by endogenous opioid peptides in the body also affects behavioral and homeostatic functions and could therefore be used to treat indications in addition to pain. Zimmerman and coworkers first described the *trans*-3,4-dimethyl-4-(3-hydroxyphenyl)piperidine μ-opioid receptor antagonists in 1978 [30] and later clarified the structural requirements that lead to higher affinity binding (Figure 11.4, A) [31]. Subsequent to the discovery of these analogs, Le Bourdonnec and coworkers designed analogs of Zimmerman's antagonists in which the rotation about the N-substituent was constrained by the formation of a fused ring [32]. Because the stereochemical requirements at C3 and C4 had been established, the 4-stereoisomers of each of the regioisomers of the constrained analogs were synthesized. Interestingly both a potent antagonist (Figure 11.4, B) and agonist (Figure 11.4, C) were found among these analogs. An analysis of the lowest energy conformers of these three molecules showed good overlap of A and B, with the hydroxyphenyl substituent in the equatorial position. The lowest energy conformer of the agonist places the hydroxyphenyl substituent in the axial position. The crystal structure of the μ-receptor was not solved until 2012 [33], and the conformationally restricted analogs were useful in gaining information about the binding pocket of the receptor prior this discovery, providing a successful complement to the traditional bioactive structures based on morphine.

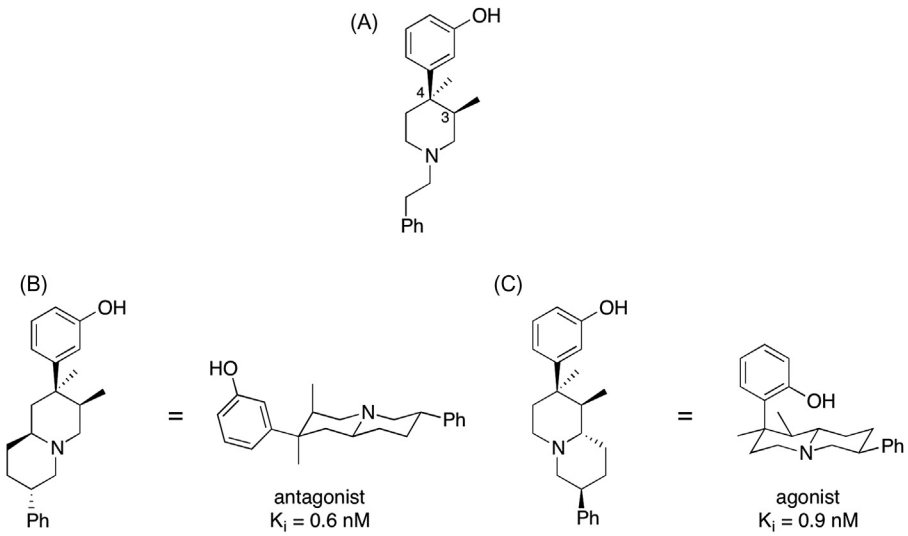

FIGURE 11.4 Structures of small molecules that interact with the μ-opioid receptor: (A) initial scaffold discovered;[30,31] (B) constrained, potent antagonist; (C) constrained, potent agonist [32].

B. Atropisomers

Atropisomers are chiral due to restricted rotations of σ-bonds with barriers exceeding 20 kcal/mol, which results in a half-life of >1000s at room temperature [34]. Atropisomers often result from a hindered rotation of bonds connecting two aromatic rings (as in Figure 11.5, A) or from a barrier in the ring flip of a medium-sized ring (as in Figure 11.5, B). Depending on the overall structure of the molecule, atropisomers can form either enantiomers or diastereomers. The first enantiomerically enriched atropisomers were isolated in 1922 [35], and since then differences in their physical properties and bioactivities have been noted [36–38].

Atropisomers racemize by a bond rotation, and the activation energy for this process depends on the electron distribution, solvent, temperature, and steric hindrance. Atropisomers that have a high barrier to racemization are easily separable and should be stable under physiological conditions. Conversely, atropisomers that have a low barrier to rotation will undergo interconversion under physiological conditions, and therefore it is unnecessary to separate them for biological activity differentiation and chemical characterization. Over the last two decades, the pharmaceutical industry has moved away from developing racemic mixtures as drug candidates; as a

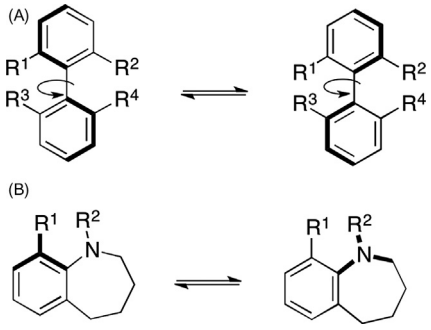

FIGURE 11.5 Generic atropisomers displaying (A) axial chirality due to hindered rotation of an aryl-aryl σ-bond and (B) planar chirality due to steric hindrance of the R groups and the dissymmetry of the bridging methylene and amine groups.

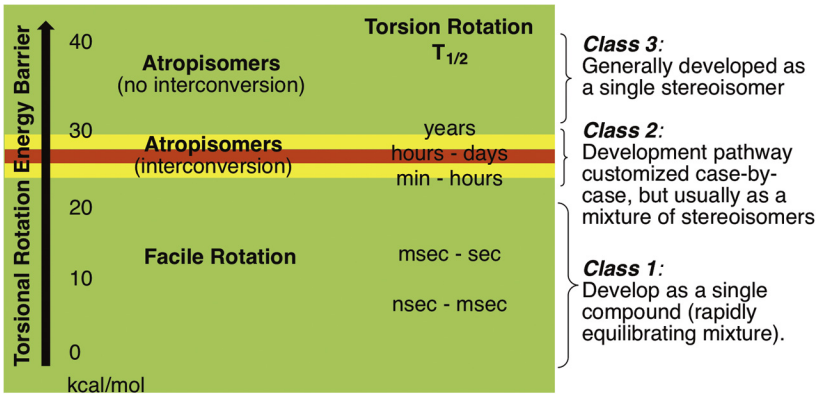

FIGURE 11.6 Table describing classes of atropisomers based on the barrier to rotation developed by LaPlante and coworkers for applications in drug development [36].

result, several reviews focus on the merits of developing a preclinical candidate as a single atropisomer rather than a mixture [36,37]. LaPlante and coworkers have established recommendations for the drug development of atropisomers based on US FDA guidelines summarized in Figure 11.6. [36,39], In short, if the barrier to rotation of an atropisomer is high ($\Delta E_{rot} \geq 30$ kcal/mol, $t_{1/2}$ in years), then the atropisomers should be resolved and the less active isomer should be treated as an impurity (Figure 11.6, Class 3). If the atropisomers rapidly equilibrate ($\Delta E_{rot} < 20$ kcal/mol, $t_{1/2}$ of minutes, Class 1), they should be treated as a single compound, since separation and individual bioactivity assessment would be challenging. The gray area of atropisomer development lies within the ΔE_{rot} 20−30 kcal/mol range ($t_{1/2}$ of hours to days, Class 2). In this area, development is challenging due to difficulties in isolation and stability, and the authors recommend increasing the ΔE_{rot} by adjusting steric hindrance, if possible, to move these compounds into Class 3.

1. *Bombesin Receptor Subtype-3 (BRS-3) agonists*

Obesity is a growing problem in our society and has been shown to cause a number of other diseases, including type-2 diabetes, cardiovascular disease, cancer, and hypertension [40]. As the rate of obesity is increasing, so too is the need for an effective anti-obesity drug. It was found that metabolic defects and obesity are present in mice that lack functional bombesin receptor subtype-3 (BRS-3) [41,42], and a BRS-3 agonist caused a decrease in food intake accompanied by an increase in metabolic rate in diet-induced obese mice [43]. In a BRS-3 HTS screen, Merck chemists discovered the compound shown in Figure 11.7 (A) [44,45]. Follow-up chemistry led to the unexpected discovery that many members of this compound class existed as a mixture of two separable enantiomers (Figure 11.7, B and C). Upon biological testing, it was determined that the *R*-enantiomer was much less potent than the *S*-enantiomer, with IC_{50} values of 169 nM versus 1.4 nM, respectively.

To determine the extent of steric bulk necessary to allow a room temperature resolution of the atropisomers, several analogs were analyzed [45]. It was found that when the C-7 substituent was either an H or F atom, no atropisomerism was observed (Figure 11.8, A). Bulkier halogens, such as Cl, a hydroxyl group (Figure 11.8, A), or a fused ring (Figure 11.8, B), led to atropisomerism. As expected, when a pyridine nitrogen atom lone pair occupied the space at the 7-position, no atropisomerism was observed (Figure 11.8, C). The addition of a large

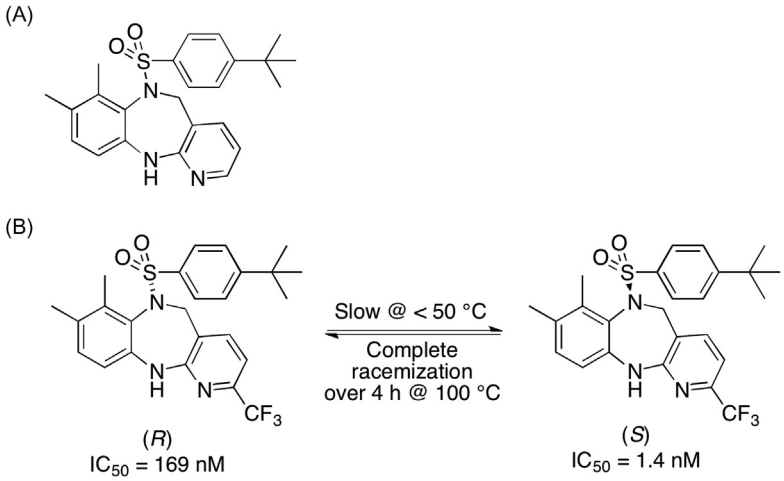

FIGURE 11.7 Structure of (A) an HTS hit from a BRS-3 screen, (B) more potent compounds resulting from follow-up chemistry that were separable atropisomers whose planar chirality was (C) confirmed by X-ray crystallography. *Adapted with permission from Liu P, Lanza TJ, Chioda M, Jones C, Chobanian HR, Guo Y, et al. Discovery of benzodiazepine sulfonamide-based bombesin receptor subtype 3 agonists and their unusual chirality. ACS Med Chem Lett 2011;2:933–7. Copyright 2011 American Chemical Society.*

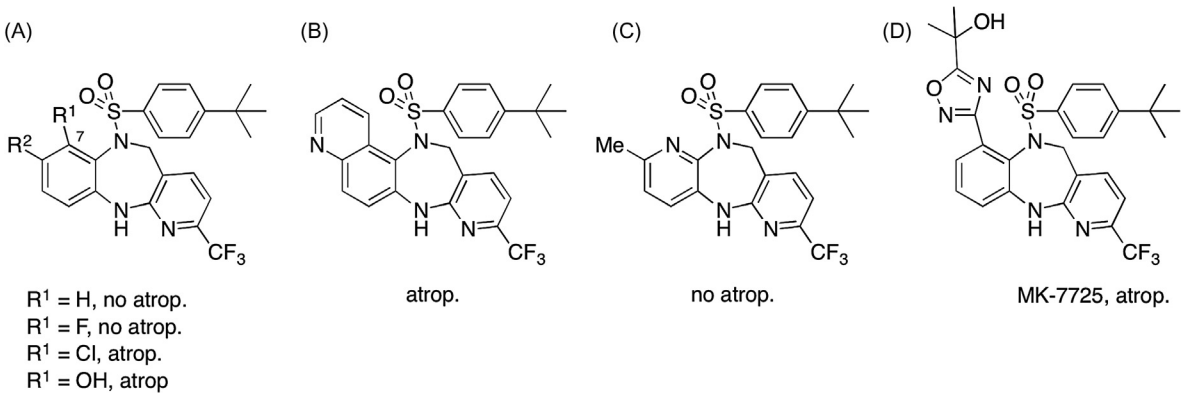

FIGURE 11.8 SAR study of atropisomers in which various substituents at C-7 were tested (no atrop. = no atropisomerism was observed; atrop. = atropisomerism was observed) [45].

heterocyclic substituent at C-7 led to the discovery of an inhibitor with comparable activity and greatly improved pharmacokinetics, MK-7725 (Figure 11.8, D). [46]

2. *Glycine transporter 1 (GlyT1) inhibitors*

Atropisomerism in the form of axial chirality is a more commonly observed occurrence, and enantiomers of this type were observed by Sugane and coworkers during their search for selective glycine transporter 1 (GlyT1) inhibitors [47]. GlyT1 is a glycine transporter that is present in forebrain areas where it terminates glycine activity by mediating its uptake [48,49]. It is believed that GlyT1 modulates NMDA receptor activity by regulating glycine levels, and a decrease in NMDA is a contributing factor to schizophrenia [50].

An HTS hit (Figure 11.9, A) from a GlyT1 screen was found to be a low micromolar inhibitor of GlyT1 but displayed no selectivity over the closely related GlyT2 [51]. It was noted that increasing the steric bulk at either the 3- or 4-position on the triazole ring increased the selectivity for GlyT1. Indeed, the *R*-enantiomer of the optimized

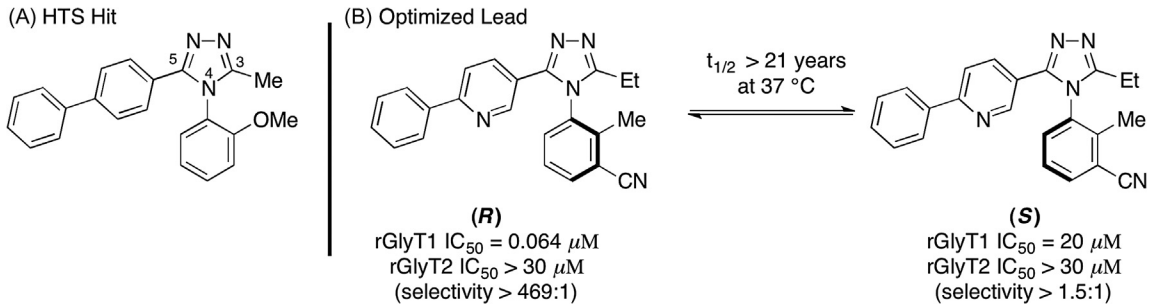

FIGURE 11.9 (A) Structure of an HTS hit from a GlyT1 screen; (B) optimized lead that resulted from increasing the steric bulk to impede axial rotation. [47].

lead (Figure 11.9, B) had an IC_{50} of 64 nM against GlyT1, while the *S*-enantiomer had an IC_{50} of 20 μM. These enantiomers were separable by chiral HPLC, and it was determined that the ΔE_{rot} was 31.4 kcal/mol (resulting in a $t_{1/2}$ of >21 years at 37°C), indicating that these compounds are Class 3 atropisomers (as described in Figure 11.6).

C. Peptidomimetics

1. *Gramicidin S Derivatives*

Gramicidin S (Figure 11.10) is a cyclic decapeptide natural product whose history spans more than seventy years. It displays antibiotic activity against both Gram-negative and Gram-positive bacteria by interacting with the bacterial lipid bilayer [52]. This interaction is closely linked to the structure of gramicidin S—its amphipathic properties are enhanced by its 3-dimensional scaffold. This enhancement is due to an antiparallel β-sheet that aligns hydrophilic and hydrophobic portions on opposite faces of the molecule. Two type II′ β-turns and four intramolecular hydrogen bonds stabilize the extended secondary structure, which has been extensively studied

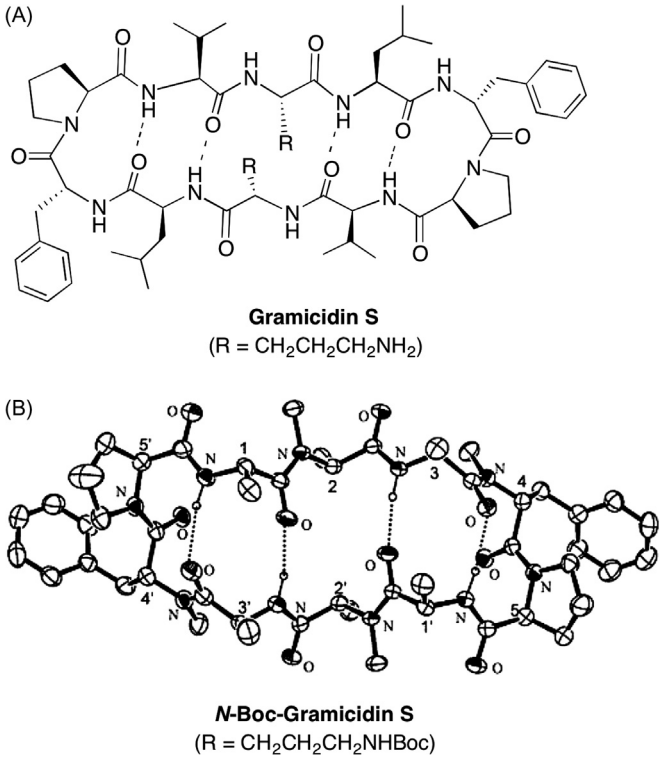

FIGURE 11.10 (A) Structure of gramicidin S showing the intramolecular hydrogen bonding that stabilizes the β-hairpin secondary structure; (B) X-ray structure of the Boc-derivative of gramicidin S [54].

by NMR [53], X-ray crystallography [54], and circular dichroism (CD) [55]. Perturbations to this 3-dimensional structure due to steric bulk or electronic variations that twist the molecule from its natural conformation cause a decrease or complete loss in function [56].

Because peptides are often plagued by poor bioavailability and rapid hydrolysis in vivo, bioisosteric replacements of the amide bond have been of great interest [57,58]. In order for such a rational design to be successful, the bioisostere must allow for a close match of the geometry of the peptide bond while remaining stable to peptidase cleavage. Among many isosteric substituents, the (*E*)-alkene peptide isosteres [58] have been quite successful, since they have a rigid geometry that is locked in place by a nonrotatable double bond and therefore mimic the sp^2 nature of the amide nitrogen particularly well. (*E*)-Alkene peptide isosteres are impervious to peptidase cleavage, but depending on the substituents attached to the double bond, any H-bonding in which an amide would participate can be lost. Furthermore, disubstituted alkenes are conformationally more flexible than the parent amide and display smaller dipole moments and greater lipophilicity. In the case of gramicidin S, loss of hydrogen bonds could be detrimental to the bioactivity, because they stabilize the molecule in its bioactive conformation. As such, this cyclopeptide antibiotic represents a useful probe substrate for the tolerance for bioisosteric group replacement and its effect on conformation and activity.

To explore the consequences of amide bond replacement on the properties of gramicidin S, more stable functional groups that should allow for the bioactive geometry of gramicidin S to remain intact were introduced into the backbone sequence. Specifically, (*E*)-alkene peptide isosteres with different substituents attached to the alkene were synthesized via a hydrozirconation/transmetalation/imine addition sequence. This synthetic sequence allowed for a stereoselective formation of the allylic amine portion of the isosteres from an alkyne and enantiomerically pure sulfinamide (Figure 11.11).

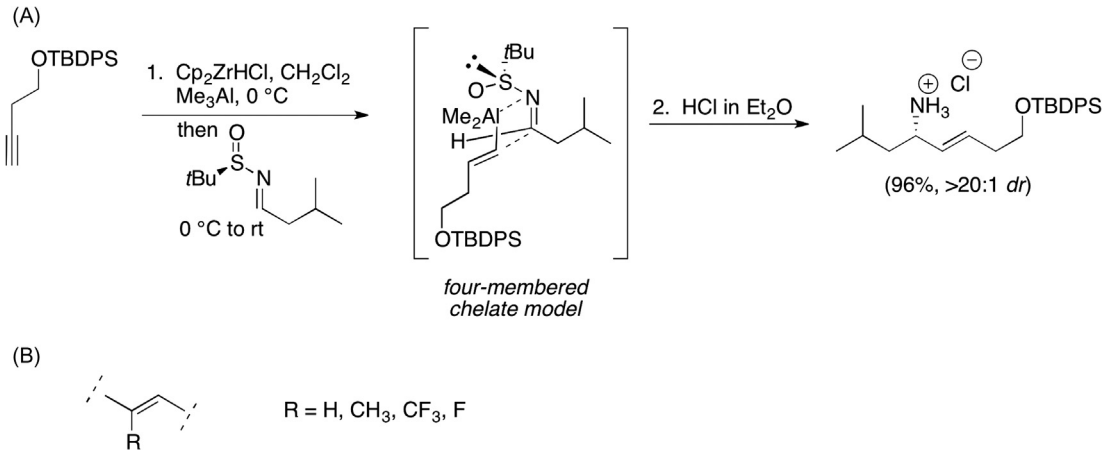

FIGURE 11.11 (A) Large-scale stereoselective synthesis of an allylic amine intermediate used in the synthesis of the (*E*)-alkene peptide isostere portion of the bioactive peptide mimic JP4-039 [59] and (B) examples of differentially substituted (*E*)-alkene peptide isosteres used in the gramicidin S analogs [60].

Trisubstituted alkenes with methyl, trifluoromethyl, and fluoro substituents as well as a disubstituted alkene were used as replacements for the Leu-Phe peptide bond. While the tertiary (*E*)-alkene peptide isostere containing the methyl substituent was of similar size as the corresponding trifluoromethyl analog, the methyl analog caused a greater perturbation of the secondary structure of the molecule, resulting in a CD spectrum that was indicative of a random coil secondary structure. The trifluoromethyl analog was a superior match of the parent compound in both solution and solid-state structures [55]. Even though the plane of the alkene was twisted 70° away from the interior of the β-turn due to the bulkiness and hydrophobicity of the CF_3 substituent, the overall geometry of the type II′ β-turn was highly preserved, and the β-hairpin structure of the cyclopeptide was unchanged.

A deprotected derivative of a trisubstituted (*E*)-alkene peptide isostere was also a successful structural mimic of the D-Phe-Pro moiety. Not only did this molecule have the desired 3-dimensional structure in solution (as indicated by the CD spectrum), but it also demonstrated equipotent biological activity to GS against *Bacillus subtilis* (20 and 15 μg/mL, respectively) [60]. The fluoro- and disubstituted (*E*)-alkene peptide isosteres also formed β-sheets, successfully mimicking the natural peptide. Therefore, these molecules demonstrate that peptide bond isostere replacements can preserve both the 3-dimensional structure as well as the biological profile of the parent structure.

2. XJB-5-131 and JP4-039 as GS-Mimics Targeting Mitochondria

Based on the properties of GS to interact with bacterial membranes and the knowledge that mitochondria evolved from bacteria, smaller and more drug-like GS-mimics were designed with the intent of using them to target the mitochondrial membrane. For the design of such a mimic, the ornithine side chains remained protected as the carbamate derivatives to decrease a potential hemolytic activity upon enrichment in erythrocytes. Furthermore, a segment of GS was used to decrease molecular weight, but the alkene peptide isostere and the D-Phe-Pro sequence were conserved to stabilize the type II′ β-turn structure, decrease the potential for proteolytic degradation, and diminish the number of hydrogen bond donors and acceptors. The (*E*)-alkene isostere XJB-5-131 was found to match a type II′ β-turn by CD analysis, and XJB-5-131 was enriched ca. 600-fold in mitochondria over the cytosol (Figure 11.12, A). The nitroxide "warhead" was introduced to react with reactive oxygen species (ROS) that are formed in the organelle, and the ROS scavenger XJB-5-131 proved to be effective in a number of disease and injury models involving cellular damage by reactive oxygen species. Such diseases include many acute and chronic degenerative disorders (e.g., hemorrhagic shock [61], hyperoxic acute lung injury [62], traumatic brain injury [63], microdialysis injury [64], and Huntington's disease [65]).

Following the success of the GS-nitroxide XJB-5-131 as a mitochondrial-targeted ROS scavenging agent, attempts to generate a lower molecular weight analog led to the discovery of JP4-039 (Figure 11.12, B). The structure of JP4-039 contains a nitroxide directly attached to the dipeptide isostere, and it also adopts a type II′ β-turn, as evidenced by its crystal structure [59]. A fluorescent derivative of JP4-039 was used to visualize the enrichment of this compound in mitochondria [66].

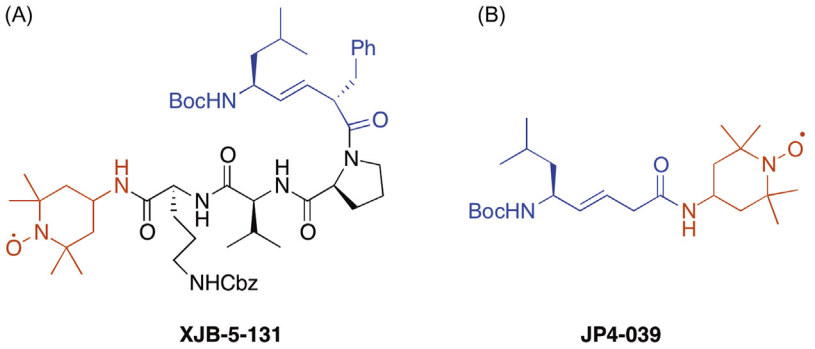

FIGURE 11.12 Structures of mitochondrial-targeted (A) XJB-5-131 and (B) JP4-039 (with the dipeptide mimetic in blue and the nitroxide in red).

D. Methyl Group Effects on Conformation

The seemingly innocuous methyl group is often added to small molecules to sterically block sites of metabolic activity and increase $t_{1/2}$. In some cases, its addition to a molecule also has a profound effect on biological potency [67,68]. Because the methyl group is a hydrophobic substituent, it can cause a slight increase in potency by reducing the desolvation energy that is required to remove the solvation by water molecules when the molecule enters a hydrophobic protein cavity from an aqueous environment [69,70]. This decrease in desolvation energy can increase the potency of a molecule by approximately 3.5-fold; any dramatic increase in potency beyond what is attributed to the increase in hydrophobicity is colloquially called the "magic methyl effect" [71] by medicinal chemists. Such "magic" effects have increased potency by over 1,000-fold [72] and even converted an agonist to an antagonist [73], but the addition of a methyl group is just as likely to decrease potency as it is to increase it [68].

1. Phospholipase D (PLD1/2) Inhibitors

Phospholipase D (PLD) catalyzes the hydrolysis of phosphatidylcholine into choline and phosphatidic acid, and suboptimal PLD function has been implicated in cancer [74] and CNS disorders [75,76]. By simply adding a methyl group to the ethylene diamine linker, Lindsley and coworkers were able to increase the activity of their PLD1 inhibitors from an IC_{50} of 11,800 nM to 20 nM (Figure 11.13) [77]. This dramatic increase in activity is likely due to a similar phenomenon observed in the factor Xa inhibitors [78]. The rotamer distribution of the dihedral angle around the amide backbone was analyzed, and it was found that when the methyl group was incorporated, fewer rotamers were formed and the rotational barriers increased. The more distinct conformational preferences favored the bioactive conformation [79].

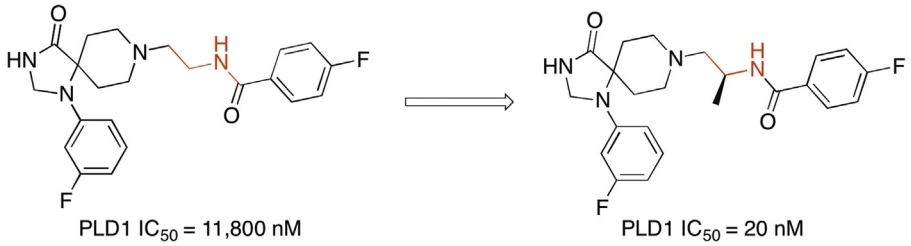

FIGURE 11.13 Dramatic effect on potency of PLD1 inhibitors by the addition of a methyl substituent, with the pertinent bonds shown in red [77].

2. *Phosphatidylinositol-3-Kinase (PI3K) Inhibitors*

While the PLD1 inhibitors experienced a dramatic increase in potency with the addition of a single methyl group, an analogous structural modification in Pfizer's phosphatidylinositol-3-kinase (PI3K) inhibitors had a much more variable effect on activity. The PI3K/mTOR (mammalian target of rapamycin) signaling pathway has been implicated in a number of disease pathologies including cancer [80] and aging [81]. Quinazolines, such as those shown in Figure 11.14 (A), were synthesized based on previously determined SAR [82]. It had been found that the C-2 methyl group was necessary for selectivity and was therefore incorporated into all new analogs. However, when a methyl group was added to the C-7 position (Figure 11.14, B), activity decreased substantially. Conversely, the addition of a methyl group at C-6 caused an almost 5-fold increase in potency over the 6-H derivative. These significant differences in potency with such seemingly small structural changes demonstrate the subtleties of relatively minor structural perturbations in medicinal chemistry. Computational studies of the 7-methyl and the 6-methyl derivatives showed that a planar orientation of the amide side-chain that was locked in place by the hydrogen bonding of the N-H to the quinazoline N-1 was optimal for the molecule to fit into the binding pocket [82]. The presence of the 7-methyl disrupts the planarity and introduces a twist to the N-C-C8-C9 dihedral angle calculated as $> 20^{\circ}$.

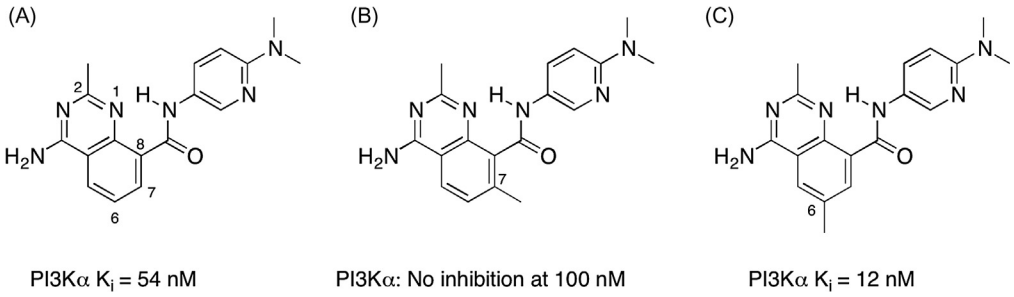

FIGURE 11.14 Structures of putative PI3K/mTOR inhibitors. The methyl group placement proved to be important for activity. (A) Absence of a methyl group at C-7 led to a fairly potent inhibitor with an IC_{50} of 54 nM, while (B) with a 7-methyl was inactive and (C) with a 6-methyl was the most potent inhibitor with an IC_{50} value of 12 nM [82].

E. Dihedral Angle Optimization

A thorough understanding of the receptor structure was used in the case of the detailed design of inhibitors of the hepatitis C virus (HCV). HCV is an infectious disease that primarily affects the liver with a chronic infection that eventually manifests itself by cirrhosis and possibly liver cancer or failure. The receptor structure of the virus was determined by a combination of X-ray crystallography of inhibitors bound to HCV NS5B, NMR spectroscopy, and docking [83]. This allowed for the detailed study of the bioactive conformation and specifically the requisite bond angles as shown in Figure 11.15 (A). Early in their studies, LaPlante and coworkers found that the bioactive conformation around dihedral angle α placed C-18 into the vicinity of NH-1. Several attempts to modulate this angle by adding a methyl group to C-16 or introducing a hydrogen-bonding pyridine N atom into the aromatic ring failed to improve potency, despite the bioactive conformation being supported by ROESY NMR correlations. Competing unfavorable forces such as electrostatic repulsion likely led to the undesirable potency. A more favorable outcome was obtained after modulating the rotation about the dihedral angles β and δ. Correlation of the cellular EC_{50} values with the substituents at C-2 showed that transitioning from the unsubstituted to a single methyl, a gem-dimethyl,

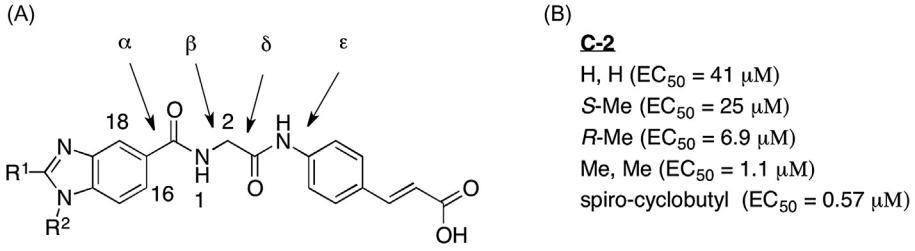

FIGURE 11.15 (A) HCV inhibitor with dihedral angles of interest highlighted and (B) EC_{50} values for varying substituents at C-2.

and finally a spiro-cyclobutyl group improved the cellular potency from 41 μM to 0.57 μM (Figure 11.15, B). Molecular mechanics was used to analyze the angle distributions of the unsubstituted C-2 compared to the spiro-cyclobutyl derivative, and the bioactive dihedral angle was more prevalent in the substituted analog.

The progression of molecular structure can be seen in Figure 11.16. The HTS hit (A) was active *in vitro* but had no cellular activity. Initial modification of the pertinent dihedral angle α led to the tryptophan series of compounds B. Unfortunately, this series had high micromolar cellular efficacy, which led to a transition to the diamide series (C). This series had the optimal dihedral angles for α, β, and δ, but still showed micromolar potency. Finally, dihedral angle ε was further restricted by the incorporation of the benzimidazole amide bond isostere as shown in D. This compound, with its fully optimized 3-dimensional structure, led to a dramatic improvement in cellular potency and served as the clinical candidate for the treatment of HCV infection.

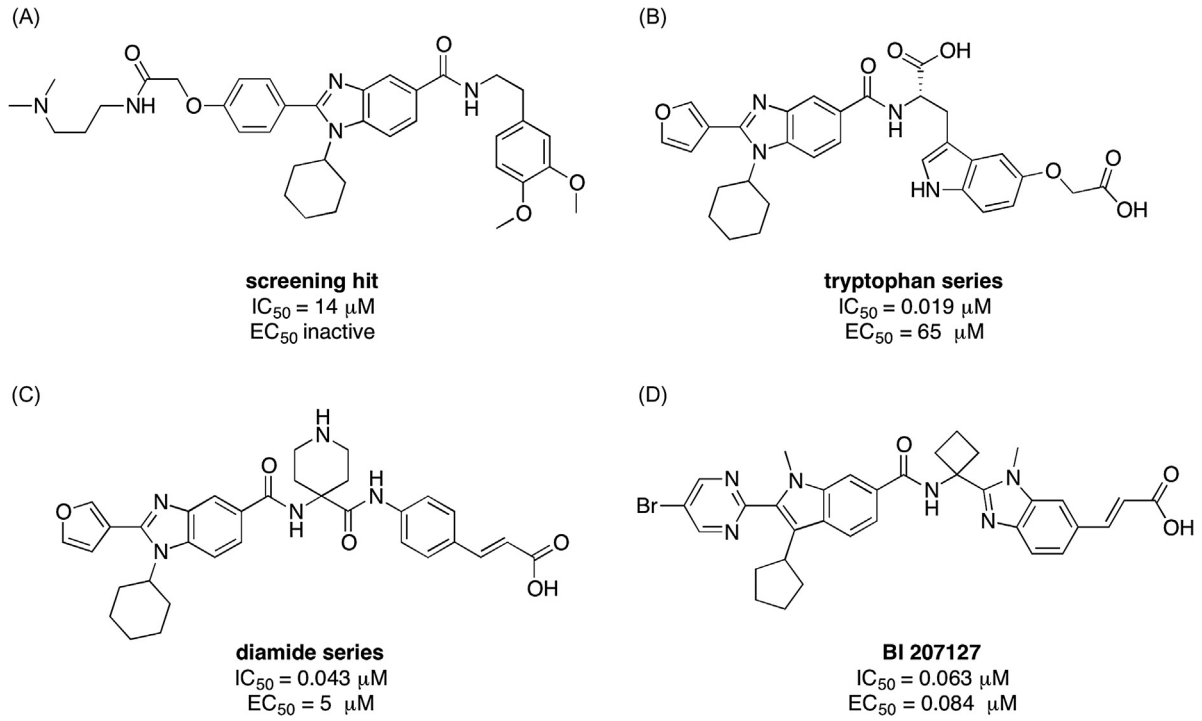

FIGURE 11.16 Structures of the (A) HTS hit, and (B) the lead structure initially used to determine bond angles, (C) the diamide series, and finally (D) the clinical candidate for HCV inhibition.

F. Diversity-Oriented Synthesis

Diversity-oriented synthesis (DOS) "involves the deliberate, simultaneous and efficient synthesis of more than one target compound in a diversity-driven approach to answer a complex problem." [84] It is a strategy that allows for the use of an efficient synthetic design to explore chemical space. This is an important as well as challenging undertaking, since chemical space is vast and significantly underexplored [85]. Estimates for the total number of synthetically tractable organic molecules containing carbon, hydrogen, nitrogen, oxygen, sulfur, and halogens limited to molecular weights below 500 g/mol vary between 10^{20} and 10^{60} molecules [86].

Two common approaches are used when applying DOS in medicinal chemistry. The first involves the expansion of a screening library so that a thorough study of functional groups, configurations, and conformations can be achieved during the primary HTS screening stage, as in the case of the β-cell apoptosis inhibitors [89]. This method offers an advanced starting point for the medicinal chemistry stage of a project, because the compounds included are so diverse yet methodical in stereochemistry and scaffold evaluation. The second approach involves the application of DOS to hit-to-lead development. Once a hit from a screen is identified, DOS can be used to synthesize a variety of structures in a targeted library rapidly to map out SAR information in a short amount of time, as demonstrated in the case of the Hsp70 inhibitors [95].

1. *Inhibitors of Cytokine-Induced β-cell Apoptosis Discovered Via HTS*

Type-1 diabetes is an autoimmune disease in which pancreatic insulin-producing β-cells undergo an increased rate of apoptosis due to an overproduction of cytokines such as IL-1β, IFN-γ, and TNF-α [87]. These cytokines activate transcription factors such as NFκB and STAT1, triggering the apoptotic pathway. An HTS screening campaign measuring cellular ATP levels as an indication of cell viability in a rat β-cell line treated with pro-inflammatory cytokines was used to find suppressors of this pathway [88]. The libraries tested in this HTS screen included several DOS libraries, among which one library was found to be particularly active. This library of fused medium-sized bicycles contained 6,488 compounds that were synthesized from stereochemically pure starting material (Figure 11.17) [89]. Starting with a chiral pool of desired amino alcohols and γ-amino acids, peptide coupling and reduction of the resulting amide were used to combine the building blocks. Acylation of the secondary amine followed by S_NAr cyclization provided the 8-membered lactam core. This synthesis utilized SynPhase solid support lanterns attached to a primary alcohol for ease of purification and handling. Capping of the aniline nitrogen by reaction with twenty-seven different building blocks, including sulfonyl chlorides, isocyanates, acyl chlorides, and aldehydes, provided a diverse set of intermediates (Figure 11.17, blue R^1). Subsequent deprotection of the secondary amine and conversion to sulfonamides, ureas, or tertiary amines yielded a diverse collection of analogs as a set of eight stereoisomers (Figure 11.17, red R^2).

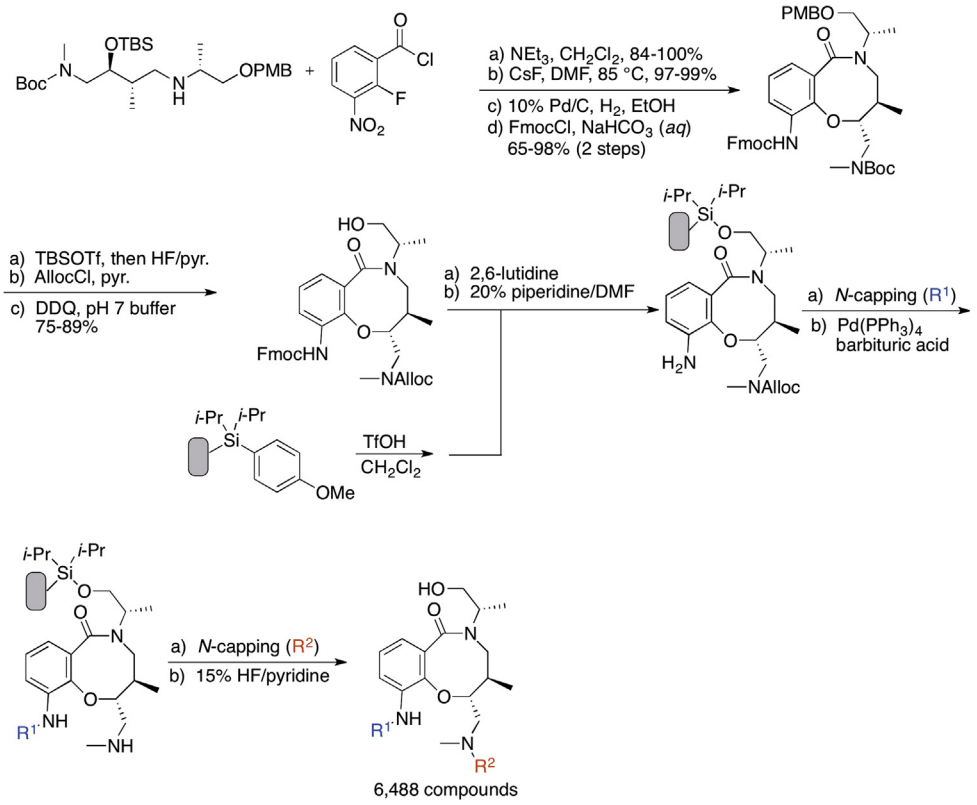

FIGURE 11.17 DOS library synthesis of 6-8 fused rings that were found to be hits in a β-cell apoptosis inhibitors screen. Only the *S,R,R* enantiomer is shown but each possible stereoisomer was synthesized. *This figure was adapted from Ref. [89].*

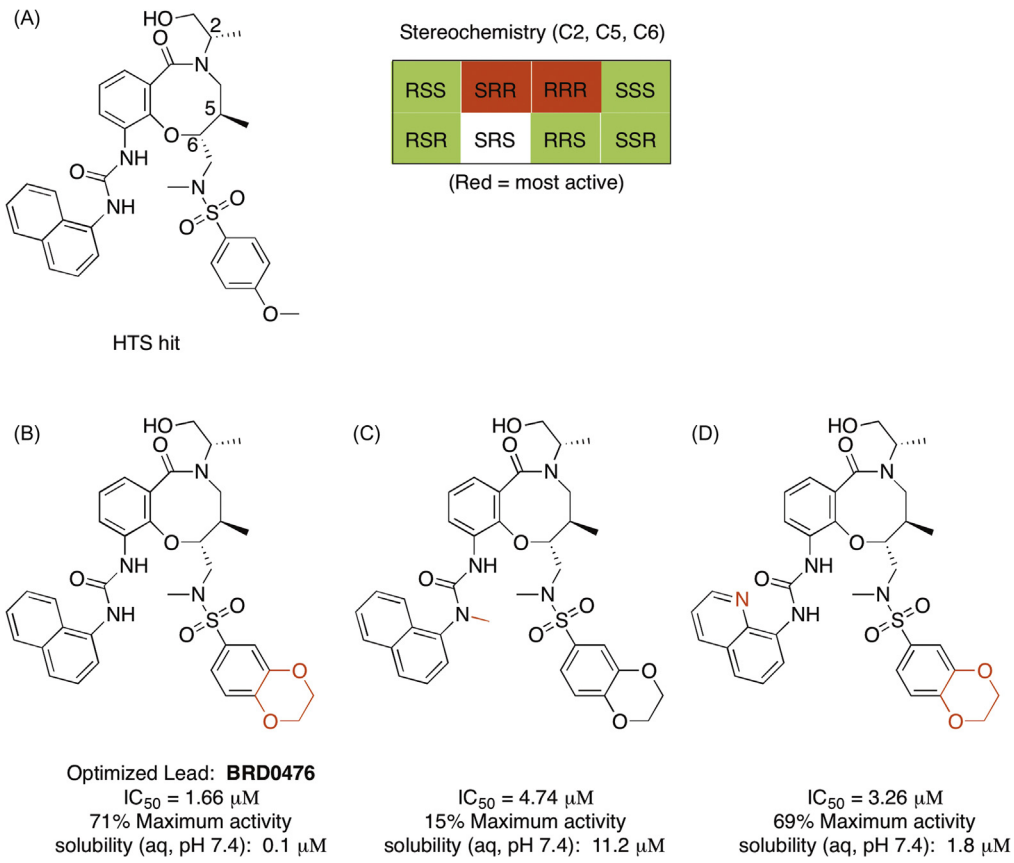

FIGURE 11.18 Structures of (A) an HTS hit and analogs with the incorporation of (B) a fused 1,4-dioxane, (C) a methyl urea, and (D) a quinoline, and their effects on potency and solubility [88,89].

The HTS screening hit is shown in Figure 11.18A. These data can be summarized in a heat map format with red boxes indicating the most active analogs and each 2×4 box showing all of the possible stereoisomers of a given analog. This heat map allows for a visualization of the activity and a graphical overview the SAR (structure-activity relationship) as well as SSAR (stereochemical structure-activity relationship) for all 6,488 analogs. The most potent compound in the original screen was the 2*S*,5*R*,6*R*-derivative with a naphthyl urea at R^1 and a *p*-methoxy phenyl sulfonamide at R^2 (Figure 11.18, A), exhibiting an EC_{50} of 4.89 μM. A comparison to other hits showed that the configuration within the 8-membered ring (C5 and C6) had a significant contribution to the activity, while the exocyclic stereocenter (C2) was inconsequential. For example, the (2*S*,5*S*,6*R*)-diastereomer of the most potent hit displayed an activity of <15% in the inhibition of apoptosis (Figure 11.18). Additionally, the bulky naphthyl urea was necessary for activity, as several analogs with smaller phenyl rings were found to be less potent.

Based on the SAR and SSAR that could be gained from the HTS, analog BRD0476 (Figure 11.18, B) was found to be the most potent suppressor of β-cell apoptosis with an IC_{50} of 1.66 μM, and it restored β-cell activity to 71 percent function. Mechanism of action studies of the optimized hit were challenging, due to the low aqueous solubility of the compound. Analogs, including a derivative with a methyl group on the urea (Figure 11.18, C), were synthesized to modify the dihedral angle between the urea and naphthyl groups. While the methyl urea analog was more soluble, its activity was only 15 percent, implying that the bulky naphthyl group was in the desired position for activity when the unsubstituted urea was used. The incorporation of a quinoline in place of the naphthyl group solved this problem, in that it allowed for the necessary steric bulk but also added a H-bonding group to increase solubility (Figure 11.18, D). Mechanism of action studies of this compound demonstrated potent inhibition of the STAT1 signal transduction induced by IFN-γ [90].

The utility of DOS in HTS screening is clearly demonstrated by this example. The information that could be gained by having so many different analogs of a core structure with all stereoisomers included allowed for the rapid determination of functional groups that were important for activity. Follow-up chemistry could focus on a single diastereomer to allow for an advanced probe in a short period of time.

2. *Molecular Probes of Heat Shock Protein 70 (Hsp70) Derived from a Focused Library*

The heat shock protein 70 (Hsp70) family forms a group of molecular chaperones that assist in the folding of nascent proteins. It also targets misfolded proteins for degradation and transport across biological membranes [91]. Hsp70s are antiapoptotic chaperones and are therefore implicated in cancer by acting at multiple points along the apoptotic pathway. Small molecules that modulate Hsp70 activity could find therapeutic applications as antitumor and antiviral agents as well as antibiotics, since viruses and bacteria also rely on the chaperones for survival. MAL3-101 [92] is an Hsp70 inhibitor that was prepared in the University of Pittsburgh Center for Chemical Methodologies and Library Development (UPCMLD) as part of a focused library based on the known Hsp70 modulator NSC 630668-R/1 [93] (Figure 11.19). MAL3-101 has fewer rotatable bonds than NSC 630668-R/1, but when the minimum energy conformations of the two compounds were superimposed via molecular modeling, the two structures overlaid well. More importantly, MAL3-101 selectively inhibited J-chaperone-stimulated Hsp70 ATPase activity in a concentration-dependent manner [92].

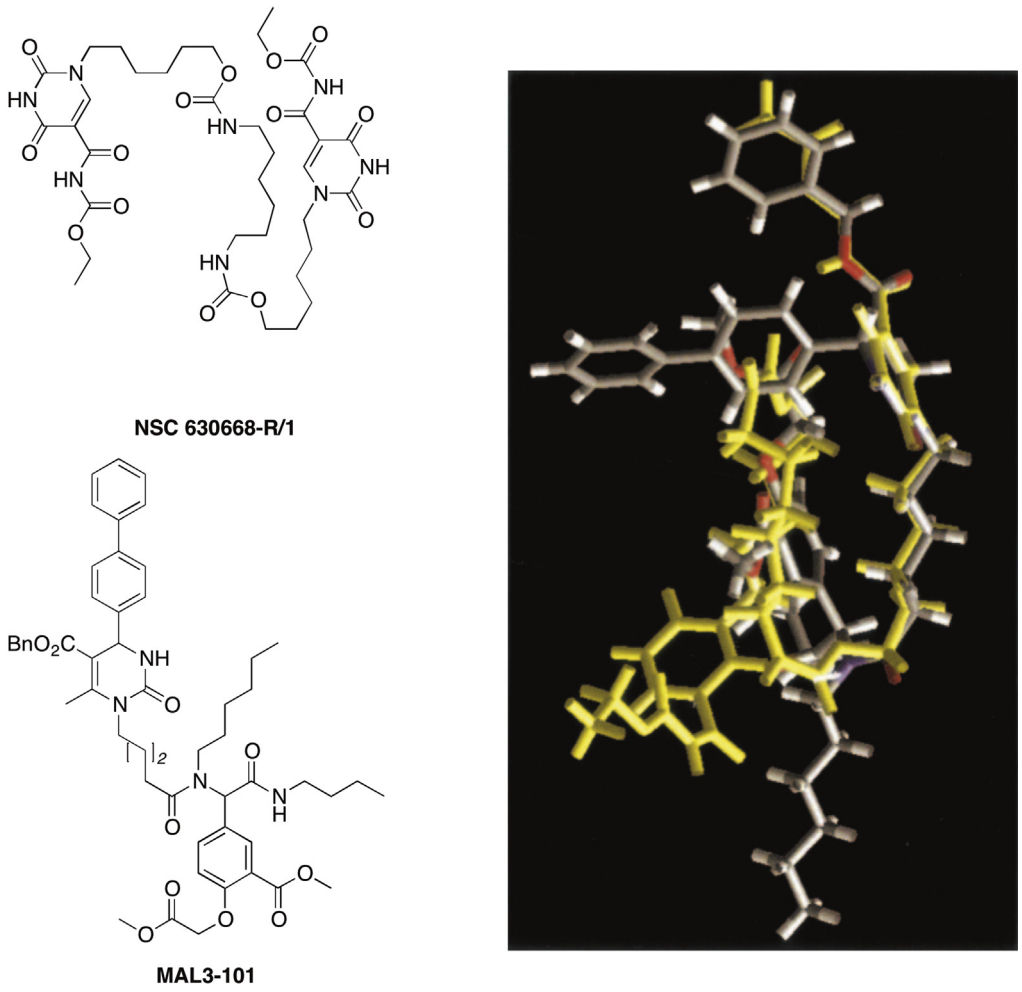

FIGURE 11.19 Superimposed structures of NSC 630668-R/1 and MAL3-101 after lowest energy conformer minimization. *This research was originally published in the Journal of Biological Chemistry: Fewell SW, Smith CM, Lyon MA, Dumitrescu TP, Wipf P, Day BW, et al. Small molecule modulators of endogenous and co-chaperone-stimulated Hsp70 ATPase activity. J Biol Chem 2004;279:51131–40. Copyright the American Society for Biochemistry and Molecular Biology.*

This library design relied on the use of two sequential multi-component reactions to synthesize efficiently analogs with seven points of diversification for screening purposes. The dihydropyrimidinones were synthesized in a one pot Biginelli reaction from the desired aldehyde, urea, and β-ketoester (Figure 11.20A), providing four points of diversification. An Ugi multi-component reaction then incorporated the appropriate amine, aldehyde, and alkyl cyanide building blocks, and contributed three additional points of diversification (Figure 11.20B).

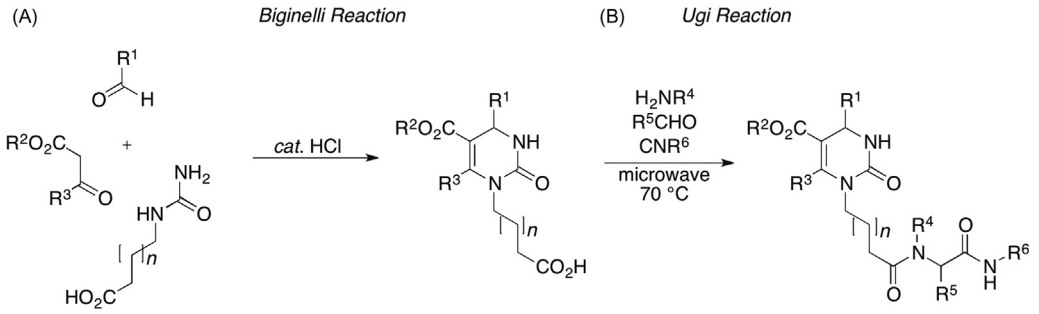

FIGURE 11.20 Diversity-oriented synthesis of the MAL3 library of Hsp70 probe molecules [94].

Following the successful discovery of MAL3-101, a second-generation library was synthesized using the same tandem Biginelli-Ugi reaction sequence [94]. In the first-generation library, it had been determined that a 5-carbon linker was optimal for Hsp70 inhibition (Figure 11.20, n = 2), and the importance of the biphenyl group in the R^1 position, the *n*-hexyl chain in the R^4 position, and the 5-formyl-2-methoxycarbonylmethoxybenzoic acid methyl ester at R^5 (Figure 11.20) were studied. This second-generation library led to the discovery of additional modulators of Hsp70 activity with diverging effects (Figure 11.21). Specifically, while MAL3-101 was an effective antimalarial, antiproliferative, and antitrypanosome agent, it had no effect on SV40. DMT3088 demonstrated improved antiproliferative activity over the first-generation analogs, and MAL2-11B showed SV40 activity (Figure 11.21), acting by inhibiting viral DNA synthesis. Interestingly, MAL2-213 had antimalarial activity but no antiproliferative activity [95]. The rapid access to conformationally more restricted NSC630668-R/1 analogs via a DOS strategy therefore allowed for the discovery of useful probes of Hsp70 with differing activities in cell proliferation, viral, and malaria assays.

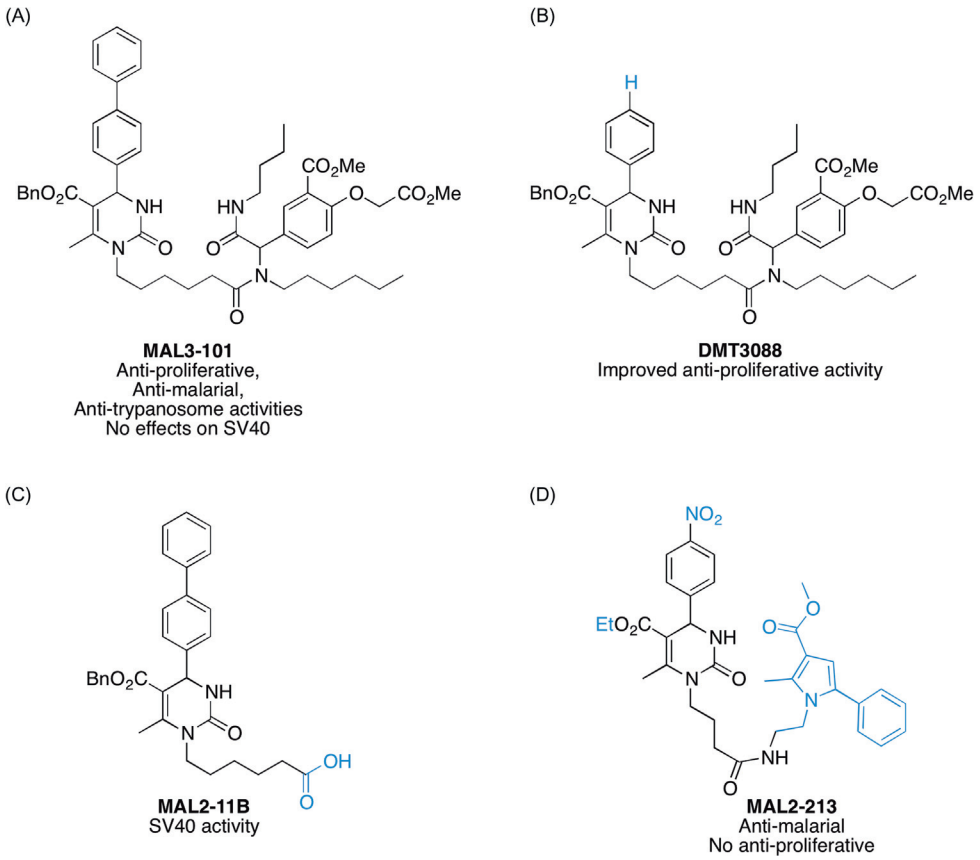

FIGURE 11.21 Differing activities of members of a focused Hsp70 library [95].

III. SUMMARY AND OUTLOOK

In biological processes, noncovalent interactions are orchestrated by complex thermodynamic principles. If a lead compound has been identified, one strategy for further optimization is to introduce structural elements that reduce the conformational flexibility, and, if possible, pre-organize the ligand in a conformation complementary to the bioreceptor. As a consequence, the energy penalty (entropic factor) associated with the binding can be diminished with respect to the flexible parent compound. This thermodynamic advantage can be leveraged into an improved value of the affinity constant. This valuable medicinal chemistry strategy based on thermodynamic considerations remains rather empirical in nature but has been successful, mainly for the optimization of preliminary pharmacophore models and the test of pharmacophore working hypotheses. Furthermore, selected structural modifications of the ligand scaffold may improve both potency and selectivity. However, the rigidification of flexible ligands without loss of potency is challenging, and sophisticated chemistry is needed to achieve the syntheses of constrained compounds with complex architectures. In this respect, the use of chemistry tools such as annulation of substituents and DOS will continue to have an important impact.

References

[1] Jencks WP. On the attribution and additivity of binding energies. Proc Natl Acad Sci 1981;78:4046–50.
[2] Raffa RB, Porreca F. Thermodynamic analysis of the drug-receptor interaction. Life Sci 1989;44:245–58.
[3] Andrews PR, Craik DJ, Martin JL. Functional group contributions to drug-receptor interactions. J Med Chem 1984;27:1648–57.
[4] Page MI. Entropy, binding energy, and enzymic catalysis. Angew Chem Int Ed Engl 1977;16:449–59.
[5] Bardi JS, Luque I, Freire E. Structure-based thermodynamic analysis of HIV-1 protease inhibitors. Biochemistry 1997;36:6588–96.
[6] Velazquez-Campoy A, Todd MJ, Freire E. HIV-1 protease inhibitors: enthalpic versus entropic optimization of the binding affinity. Biochemistry 2000;39:2201–7.
[7] Searle MS, Williams DH. The cost of conformational order: entropy changes in molecular associations. J Am Chem Soc 1992;114:10690–7.
[8] Williams DH, Westwell MS. Aspects of weak interactions. Chem Soc Rev 1998;27:57–64.
[9] Williams DH, Stephens E, O'Brien DP, Zhou M. Understanding noncovalent interactions: Ligand binding energy and catalytic efficiency from ligand-induced reductions in motion within receptors and enzymes. Angew Chem Int Ed 2004;43:6596–616.
[10] Böhm H-J. The development of a simple empirical scoring function to estimate the binding constant for a protein-ligand complex of known three-dimensional structure. J Comput Aided Mol Des 1994;8:243–56.
[11] Dunitz JD. Win some, lose some: enthalpy-entropy compensation in weak intermolecular interactions. Chem Biol 1995;2:709–12.
[12] Gilli P, Ferretti V, Gilli G, Borea PA. Enthalpy-entropy compensation in drug-receptor binding. J Phys Chem 1994;98:1515–18.
[13] Velazquez-Campoy A, Luque I, Freire E. The application of thermodynamic methods in drug design. Thermochim Acta 2001;380:217–27.
[14] Weiland GA, Minneman KP, Molinoff PB. Fundamental difference between the molecular interactions of agonists and antagonists with the beta-adrenergic receptor. Nature 1979;281:114–17.
[15] Miklavc A, Kocjan D, Mavri J, Koller J, Hadzi D. On the fundamental difference in the thermodynamics of agonist and antagonist interactions with β-adrenergic receptors and the mechanism of entropy-driven binding. Biochem Pharmacol 1990;40:663–9.
[16] Borea PA, Dalpiaz A, Varani K, Guerra L, Gilli G. Binding thermodynamics of adenosine A2a receptor ligands. Biochem Pharmacol 1995;49:461–9.
[17] Davis AM, Teague SJ. Hydrogen bonding, hydrophobic interactions, and failure of the rigid receptor hypothesis. Angew Chem Int Ed 1999;38:736–49.
[18] Hruby VJ, Li G, Haskell-Luevano C, Shenderovich M. Design of peptides, proteins, and peptidomimetics in chi space. Peptide Sci 1997;43:219–66.
[19] Gardiner J, Abell AD. Synthesis and solid-state conformation of phenylalanine mimetics constrained in a proline-like conformation. Org Biomol Chem 2004;2:2365–70.
[20] Gibson SE, Jones JO, McCague R, Tozer MJ, Whitcombe NJ. A bromoarene based approach to phenylalanine analogues Hic and Nic. Synlett 1999;954–6.
[21] Hanessian S, Bernstein N, Yang R-Y, Maguire R. Asymmetric synthesis of l-azetidine-2-carboxylic acid and 3-substituted congener–conformationally constrained analogs of phenylalanine, naphthylalanine, and leucine. Bioorg Med Chem Lett 1999;9:1437–42.
[22] Cativiela C, Lasa M, López P. Synthesis of enantiomerically pure cis- and trans-cyclopentane analogues of phenylalanine. Tetrahedron Asymmetry 2005;16:2613–23.
[23] Pujadas G, Vaque M, Ardevol A, Blade C, Salvado MJ, Blay M, et al. Protein–ligand docking: a review of recent advances and future perspectives. Curr Pharm Anal 2008;4:1–19.
[24] Kim R, Skolnick J. Assessment of programs for ligand binding affinity prediction. J Comput Chem 2008;29:1316–31.
[25] Gao C, Park M-S, Stern HA. Accounting for ligand conformational restriction in calculations of protein-ligand binding affinities. Biophys J 2010;98:901–10.
[26] Nicklaus MC, Wang S, Driscoll JS, Milne GWA. Conformational changes of small molecules binding to proteins. Bioorg Med Chem 1995;3:411–28.
[27] Veber DF, Johnson SR, Cheng H-Y, Smith BR, Ward KW, Kopple KD. Molecular properties that influence the oral bioavailability of drug candidates. J Med Chem 2002;45:2615–23.
[28] Lipinski CA, Lombardo F, Dominy BW, Feeney PJ. Experimental and computational approaches to estimate solubility and permeability in drug discovery and development settings. Adv Drug Deliv Rev 1997;23:3–25.

[29] Varma MVS, Obach RS, Rotter C, Miller HR, Chang G, Steyn SJ, et al. Physicochemical space for optimum oral bioavailability: Contribution of human intestinal absorption and first-pass elimination. J Med Chem 2010;53:1098–108.
[30] Zimmerman DM, Leander JD, Cantrell BE, Reel JK, Snoddy J, Mendelsohn LG, et al. Structure-activity relationships of trans-3,4-dimethyl-4-(3-hydroxyphenyl)piperidine antagonists for μ- and κ-opioid receptors. J Med Chem 1993;36:2833–41.
[31] Zimmerman DM, Nickander R, Horng JS, Wong DT. New structural concepts for narcotic antagonists defined in a 4-phenylpiperidine series. Nature 1978;275:332–4.
[32] Le Bourdonnec B, Goodman AJ, Michaut M, Ye H-F, Graczyk TM, Belanger S, et al. Elucidation of the bioactive conformation of the n-substituted trans-3,4-dimethyl-4-(3-hydroxyphenyl)piperidine class of μ-opioid receptor antagonists. J Med Chem 2006;49:7278–89.
[33] Manglik A, Kruse AC, Kobilka TS, Thian FS, Mathiesen JM, Sunahara RK, et al. Crystal structure of the μ-opioid receptor bound to a morphinan antagonist. Nature 2012;485:321–6.
[34] Ōki M. Recent advances in atropisomerism N.p. In: Allinger NL, Eliel EL, Wilen SH, editors. Topics in stereochemistry, vol. 14. John Wiley & Sons, Inc; 1983. p. 1–81
[35] Christie GH, Kenner J. LXXI: the molecular configurations of polynuclear aromatic compounds. Part I. The resolution of γ-6 : 6′-dinitro- and 4 : 6 : 4′ : 6′-tetranitro-diphenic acids into optically active components. J Chem Soc Trans 1922;121:614–20.
[36] LaPlante SR, Edwards PJ, Fader LD, Jakalian A, Hucke O. Revealing atropisomer axial chirality in drug discovery. Chem Med Chem 2011;6:505–13.
[37] LaPlante SR, Fader LD, Fandrick KR, Fandrick DR, Hucke O, Kemper R, et al. Assessing atropisomer axial chirality in drug discovery and development: natural products and drugs. Chirality 2011;25:265–74.
[38] Zask A, Murphy J, Ellestad GA. Biological stereoselectivity of atropisomeric natural products and drugs. Chirality 2013;25:265–74.
[39] Food and Drug Administration. Policy statement on the development of new stereoisomeric drugs. Available from: <http://www.fda.gov/drugs/GuidanceComplianceRegulatoryInformation/Guidances/ucm122883.htm>; 2011 [accessed 13.10.20].
[40] Olshansky SJ, Passaro DJ, Hershow RC, Layden J, Carnes BA, Brody J, et al. A potential decline in life expectancy in the United States in the 21st century. N Engl J Med 2005;352:1138–45.
[41] Ohki-Hamazaki H, Watase K, Yamamoto K, Ogura H, Yamano M, Yamada K, et al. Mice lacking bombesin receptor subtype-3 develop metabolic defects and obesity. Nature 1997;390:165–9.
[42] Ladenheim EE, Hamilton NL, Behles RR, Bi S, Hampton LL, Battey JF, et al. Factors contributing to obesity in bombesin receptor subtype-3-deficient mice. Endocrinology 2008;149:971–8.
[43] Guan X-M, Chen H, Dobbelaar PH, Dong Y, Fong TM, Gagen K, et al. Regulation of energy homeostasis by bombesin receptor subtype-3: selective receptor agonists for the treatment of obesity. Cell Metab 2010;11:101–12.
[44] Welch CJ, Gong X, Schafer W, Chobanian H, Lin L, Biba M, et al. Factors influencing the interconversion of a new class of dibenzodiazepine sulfonamide atropisomers. Chirality 2009;21:E105–9.
[45] Liu P, Lanza TJ, Chioda M, Jones C, Chobanian HR, Guo Y, et al. Discovery of benzodiazepine sulfonamide-based bombesin receptor subtype 3 agonists their unusual chirality. ACS Med Chem Lett 2011;2:933–7.
[46] Chobanian HR, Guo Y, Liu P, Chioda M, Lanza TJ, Chang L, et al. Discovery of MK-7725, a potent, selective bombesin receptor subtype-3 agonist for the treatment of obesity. ACS Med Chem Lett 2012;3:252–6.
[47] Sugane T, Tobe T, Hamaguchi W, Shimada I, Maeno K, Miyata J, et al. Atropisomeric 4-phenyl-4H-1,2,4-triazoles as selective glycine transporter 1 inhibitors. J Med Chem 2013;56:5744–56.
[48] Bröer S, Cavanaugh JA, Rasko JEJ. Neutral amino acid transport in epithelial cells and its malfunction in Hartnup disorder. Biochem Soc Trans 2005;33:233–6.
[49] Sur C, Kinney GG. Glycine transporter 1 inhibitors and modulation of NMDA receptor-mediated excitatory neurotransmission. Curr Drug Targets 2007;8:643–9.
[50] Danysz W, Parsons CG. Glycine and N-methyl-D-aspartate receptors: physiological significance and possible therapeutic applications. Pharmacol Rev 1998;50:597–664.
[51] Sugane T, Tobe T, Hamaguchi W, Shimada I, Maeno K, Miyata J, et al. Synthesis and biological evaluation of 3-biphenyl-4-yl-4-phenyl-4H-1,2,4-triazoles as novel glycine transporter 1 inhibitors. J Med Chem 2011;54:387–91.
[52] Gause GF, Brazhnikova MG. Gramicidin S. and its use in the treatment of infected wounds. Nature 1944;154:703.
[53] Stern A, Gibbons WA, Craig LC. A conformational analysis of gramicidin S-A by nuclear magnetic resonance. Proc Natl Acad Sci 1968;61:734–41.
[54] Yamada K, Unno M, Kobayashi K, Oku H, Yamamura H, Araki S, et al. Stereochemistry of protected ornithine side chains of gramicidin S derivatives: X-ray crystal structure of the bis-Boc-tetra-N-methyl derivative of gramicidin S. J Am Chem Soc 2002;124:12684–8.
[55] Xiao J, Weisblum B, Wipf P. Electrostatic versus steric effects in peptidomimicry: synthesis and secondary structure analysis of gramicidin S analogues with (E)-alkene peptide isosteres. J Am Chem Soc 2005;127:5742–3.
[56] Grotenbreg GM, Kronemeijer M, Timmer MSM, El Oualid F, van Well RM, Verdoes M, et al. A practical synthesis of gramicidin S and sugar amino acid containing analogues. J Org Chem 2004;69:7851–9.
[57] Wipf P, Xiao J, Stephenson CRJ. Peptide-like molecules (plms): a journey from peptide bond isosteres to gramicidin S mimetics and mitochondrial targeting agents. Chimia 2009;63:764–75.
[58] Skoda EM, Davis GC, Wipf P. Allylic amines as key building blocks in the synthesis of (E)-alkene peptide isosteres. Org Process Res Develop 2012;16:26–34.
[59] Frantz M-C, Pierce JG, Pierce JM, Kangying L, Qingwei W, Johnson M, et al. Large-scale asymmetric synthesis of the bioprotective agent JP4-039 and analogs. Org Lett 2011;13:2318–21.
[60] Xiao J, Weisblum B, Wipf P. Trisubstituted (E)-alkene dipeptide isosteres as β-turn promoters in the gramicidin S cyclodecapeptide scaffold. Org Lett 2006;8:4731–4.
[61] Fink MP, Macias CA, Xiao J, Tyurina YY, Jiang J, Belikova N, et al. Hemigramicidin-TEMPO conjugates: novel mitochondria-targeted anti-oxidants. Biochem Pharmacol 2007;74:801–9.

[62] Tyurina YY, Tyurin VA, Kaynar AM, Kapralova VI, Wasserloos K, Li J, et al. Oxidative lipidomics of hyperoxic acute lung injury: mass spectrometric characterization of cardiolipin and phosphatidylserine peroxidation. Am J Physiol 2010;299:L73–85.
[63] Ji J, Kline AE, Amoscato A, Samhan-Arias AK, Sparvero LJ, Tyurin VA, et al. Lipidomics identifies cardiolipin oxidation as a mitochondrial target for redox therapy of brain injury. Nat Neurosci 2012;15:1407–13.
[64] Nesbitt KM, Jaquins-Gerstl A, Skoda EM, Wipf P, Michael AC. Pharmacological mitigation of tissue damage during brain microdialysis. Analyt Chem 2013;85:8173–9.
[65] Xun Z, Rivera-Sánchez S, Ayala-Peña S, Lim J, Budworth H, Skoda EM, et al. Targeting of XJB-5-131 to mitochondria suppresses oxidative DNA damage and motor decline in a mouse model of Huntington's disease. Cell Rep 2012;2:1137–42.
[66] Frantz M-C, Skoda EM, Sacher JR, Epperly MW, Goff JP, Greenberger JS, et al. Synthesis of analogs of the radiation mitigator JP4-039 and visualization of BODIPY derivatives in mitochondria. Org Biomol Chem 2013;11:4147–53.
[67] Barreiro EJ, Kümmerle AE, Fraga CAM. The methylation effect in medicinal chemistry. Chem Rev 2011;111:5215–46.
[68] Leung CS, Leung SSF, Tirado-Rives J, Jorgensen WL. Methyl effects on protein–ligand binding. J Med Chem 2012;55:4489–500.
[69] Némethy G. Hydrophobe wechselwirkungen [Hydrophobic interactions]. Angew Chem 1967;79:260–71 [in German].
[70] Southall NT, Dill KA, Haymet ADJ. A view of the hydrophobic effect. J Phys Chem B 2001;106:521–33.
[71] Schönherr H, Cernak T. Profound methyl effects in drug discovery and a call for new C-H methylation reactions. Angew Chem Int Ed 2013;52:12256–67.
[72] Quancard J, Bollbuck B, Janser P, Angst D, Berst F, Buehlmayer P, et al. A potent and selective S1P1 antagonist with efficacy in experimental autoimmune encephalomyelitis. Chem Biol 2012;19:1142–51.
[73] Goodman AJ, Le Bourdonnec B, Dolle RE. Mu opioid receptor antagonists: recent developments. Chem Med Chem 2007;2:1552–70.
[74] Jenkins GM, Frohman MA. Phospholipase D: a lipid centric review. Cell Mol Life Sci 2005;62:2305–16.
[75] Elvers M, Stegner D, Hagedorn I, Kleinschnitz C, Braun A, Kuijpers MEJ, et al. Impaired αIIbβ3 integrin activation and shear-dependent thrombus formation in mice lacking phospholipase D1. Sci Signal 2010;3:1–10.
[76] Oliveira TG, Chan RB, Tian H, Laredo M, Shui G, Staniszewski A, et al. Phospholipase D2 ablation ameliorates Alzheimer's disease-linked synaptic dysfunction and cognitive deficits. J Neurosci 2010;30:16419–28.
[77] O'Reilly MC, Scott SA, Brown KA, Oguin TH, Thomas PG, Daniels JS, et al. Development of dual PLD1/2 and PLD 2 selective inhibitors from a common 1,3,8-triazaspiro[4.5]decane core: discovery of ML298 and ML299 that decrease invasive migration in U87-MG glioblastoma cells. J Med Chem 2013;56:2695–9.
[78] Czekaj M, Klein SI, Guertin KR, Gardner CJ, Zulli AL, Pauls HW, et al. Optimization of the β-aminoester class of factor Xa inhibitors. Part 1: P4 and side-chain modifications for improved in vitro potency. Bioorg Med Chem Lett 2002;12:1667–70.
[79] Schärfer C, Schulz-Gasch T, Ehrlich H-C, Guba W, Rarey M, Stahl M. Torsion angle preferences in druglike chemical space: a comprehensive guide. J Med Chem 2013;56:2016–28.
[80] Engelman JA, Luo J, Cantley LC. The evolution of phosphatidylinositol 3-kinases as regulators of growth and metabolism. Nat Rev Genet 2006;7:606–19.
[81] Fontana L, Partridge L, Longo VD. Extending healthy life span-from yeast to humans. Science 2010;328:321–6.
[82] Liu KKC, Huang X, Bagrodia S, Chen JH, Greasley S, Cheng H, et al. Quinazolines with intra-molecular hydrogen bonding scaffold (iMHBS) as PI3K/mTOR dual inhibitors. Bioorg Med Chem Lett 2011;21:1270–4.
[83] LaPlante SR, Gillard JR, Jakalian A, Aubry N, Coulombe R, Brochu C, et al. Importance of ligand bioactive conformation in the discovery of potent indole-diamide inhibitors of the Hepatitis C virus NS5B. J Am Chem Soc 2010;132:15204–12.
[84] Spring DR. Diversity-oriented synthesis: a challenge for synthetic chemists. Org Biomol Chem 2003;1:3867–70.
[85] Virshup AM, Contreras-García J, Wipf P, Yang W, Beratan DN. Stochastic voyages into uncharted chemical space produce a representative library of all possible drug-like compounds. J Am Chem Soc 2013;135:7296–303.
[86] Fink T, Bruggesser H, Reymond J-L. Virtual exploration of the small-molecule chemical universe below 160 daltons. Angew Chem Int Ed 2005;44:1504–8.
[87] Cnop M, Welsh N, Jonas J-C, Jörns A, Lenzen S, Eizirik DL. Mechanisms of pancreatic β-cell death in type 1 and type 2 diabetes: many differences, few similarities. Diabetes 2005;54:S97–107.
[88] Chou DH-C, Bodycombe NE, Carrinski HA, Lewis TA, Clemons PA, Schreiber SL, et al. Small-molecule suppressors of cytokine-induced β-cell apoptosis. ACS Chem Biol 2010;5:729–34.
[89] Chou DH-C, Duvall JR, Gerard B, Liu H, Pandya BA, Suh B-C, et al. Synthesis of a novel suppressor of β-cell apoptosis via diversity-oriented synthesis. ACS Med Chem Lett 2011;2:698–702.
[90] Scully SS, Tang AJ, Lundh M, Mosher CM, Perkins KM, Wagner BK. Small-molecule inhibitors of cytokine-mediated STAT1 signal transduction in β-cells with improved aqueous solubility. J Med Chem 2013;56:4125–9.
[91] Hartl FU. Molecular chaperones in cellular protein folding. Nature 1996;381:571–80.
[92] Fewell SW, Smith CM, Lyon MA, Dumitrescu TP, Wipf P, Day BW, et al. Small molecule modulators of endogenous and co-chaperone-stimulated Hsp70 ATPase activity. J Biol Chem 2004;279:51131–40.
[93] Fewell SW, Day BW, Brodsky JL. Identification of an inhibitor of Hsc70-mediated protein translocation and ATP hydrolysis. J Biol Chem 2001;276:910–14.
[94] Werner S, Turner DM, Lyon MA, Huryn DM, Wipf P. A focused library of tetrahydropyrimidinone amides via a tandem Biginelli-Ugi multi-component process. Synlett 2006;14:2334–8.
[95] Huryn DM, Brodsky JL, Brummond KM, Chambers PG, Eyer B, Ireland AW, et al. Chemical methodology as a source of small-molecule checkpoint inhibitors and heat shock protein 70 (Hsp70) modulators. Proc Natl Acad Sci 2011;108:6757–62.